TISSUE ENGINEERING: Part A
Volume 20, Numbers 11 and 12, 2014

DOI: 10.1089/ten.tea.2013.0245

The Dominant Role of *IL-8* as an Angiogenic Driver in a Three-Dimensional Physiological Tumor Construct for Drug Testing

Pamela H.S. Tan, PhD,[1] Su Shin Chia, BEng,[1] Siew Lok Toh, PhD,[1] James C.H. Goh, PhD,[1] and Saminathan Suresh Nathan, MD[2]

The induction of angiogenesis and the promotion of tumor growth and invasiveness are processes critical to metastasis, and are dependent on reciprocal interactions between tumor cells and their microenvironment. The formation of a clinically relevant tumor requires support from the surrounding stroma, and it is hypothesized that three-dimensional (3D) tumor coculture models offer a microenvironment that more closely resembles the physiological tumor microenvironment. In this study, we investigated the effects of tissue-engineered 3D architecture and tumor–stroma interaction on the angiogenic factor secretion profiles of U2OS osteosarcoma cells by coculturing the tumor cells with immortalized fibroblasts or human umbilical vein endothelial cells (HUVECs). We also carried out Transwell® migration assays for U2OS cells grown in monoculture or fibroblast coculture systems to study the physiological effect of upregulated angiogenic factors on endothelial cell migration. Anti-IL-8 and anti-vascular endothelial growth factor (VEGF)-A therapies were tested out on these models to investigate the role of 3D culture and the coculture of tumor cells with immortalized fibroblasts on the efficacy of antiangiogenic treatments. The coculture of U2OS cells with immortalized fibroblasts led to the upregulation of *IL-8* and VEGF-A, especially in 3D culture. Conversely, coculture with endothelial cells resulted in the downregulation of VEGF-A for cells seeded in 3D scaffolds. The migration of HUVECs through the Transwell polycarbonate inserts increased for the 3D and immortalized fibroblast coculture models, and the targeted inhibition of *IL-8* greatly reduced HUVEC migration despite the presence of VEGF-A. A similar effect was not observed when anti-VEGF-A neutralizing antibody was used instead, suggesting that *IL-8* plays a more critical role in endothelial cell migration than VEGF-A, with significant implications on the clinical utility of antiangiogenic therapy targeting VEGF-A.

Introduction

In vitro tumor cell culture systems have been widely used as preclinical models for drug testing. Although three-dimensional (3D) models are gradually being introduced to the field, very few have been able to mimic the heterogeneous tumor–stroma interaction of the tumor microenvironment. The interactions between tumor cells and their supporting stroma increase cancer aggressiveness through several mechanisms, with the induction of angiogenesis being one of the most important.[1] It is hypothesized that 3D tumor coculture models offer a microenvironment that more closely resembles the physiological tumor microenvironment, while the resulting upregulated angiogenic factors stimulate endothelial cell migration.

Established strategies from tissue engineering can be exploited to investigate the dynamic role of chemical, cell–cell, cell–extracellular matrix (ECM), and mechanical interactions in the pathogenesis of cancer.[2–5] Biodegradable 3D engineered scaffolds commonly used in tissue engineering are capable of mimicking the ECM and providing structural support to the seeded tumor cells.[3] These engineered scaffolds have great potential in recreating the natural environment of living tissue, and are able to promote the signaling pathways for cellular migration, proliferation, and differentiation.[6] Poly(α-hydroxyacids) are very popular and have been fabricated into 3D scaffolds via a wide range of techniques.[7,8] However, poly(α-hydroxyacids) tend to degrade by bulk erosion, which could lead to the release of high concentrations of α-hydroxyacids and cause the acidification of the culture medium. This is of concern as even nontoxic concentrations have been shown to lead to a decrease in cell proliferation and rapid cell differentiation.[9] Silk fibers are comprised of fibroin, a filament core protein,

[1]Tissue Repair Laboratory, Department of Bioengineering, National University of Singapore, Singapore, Singapore.
[2]Musculoskeletal Oncology Research Laboratories, Department of Orthopaedic Surgery, National University of Singapore, Singapore, Singapore.

and a glue-like coating of sericin proteins. Silk fibroin is a natural polymer and has been widely used clinically as sutures.[10,11] Silk fibroin has good biocompatibility, is permeable to oxygen and water, has relatively low thrombogenicity, and has good cell adhesion and growth characteristics.[12] It can also be easily processed and surface modified for tissue engineering applications, and has been established for use in the development of breast and prostate cancer models; thus, it is suitable for the fabrication of biomimetic tumor constructs.[13–18] Silk is classified into mulberry and nonmulberry types. We have chosen mulberry silk from *Bombyx mori* silk worms, which are easily domesticated, ubiquitous in distribution, and well-characterized, unlike nonmulberry silkworms that are wild and heterogeneous, resulting in batch-to-batch variability.[19] We fabricated a porous sponge with degummed *Bombyx mori* silk and seeded it with osteosarcoma cell lines to form the 3D tumor construct. Our previous work showed that *Bombyx mori* silk as a strata is nontoxic and does not confer any difference to proliferation-related or angiogenesis-related factors in tumor cells when compared to tissue culture polystyrene.[14]

Multiple cell types interact directly in 3D microenvironments *in vivo* via heterotypic cell–cell junctions or paracrine-mediated signaling mechanisms. Interactions between cancer cells and their supporting stroma result in increased growth and invasiveness, and also contribute to the formation of drug-resistant phenotypes.[20–22] Fibroblasts are the major constituent of the stroma and are responsible for the secretion of increased levels of ECM proteins, growth factors, and chemotactic factors to coordinate the migration of inflammatory cells and vascular progenitor cells *in vivo*. Fibroblasts also supply the scaffold structure for cell growth and proliferation.[23–25] Cancer-associated fibroblasts are the main cellular component of the tumor stroma and provide additional oncogenic signals that enhance the proliferation and invasion of cancer cells.[26,27] Angiogenesis is fundamental to tumor growth, progression, and metastasis. A critical step in this process is the outgrowth of endothelial cells from preexisting capillary vessels and their migration toward the tumor cells under the stimulation of angiogenic growth factors.[28,29] Circulating endothelial progenitor cells have been found to play a crucial role in sustaining angiogenesis in both primary and metastatic tumors,[30] and high levels of angiogenic factor production have been associated with advanced tumor staging and poor prognosis.[31–33]

Vascular endothelial growth factor (VEGF)-A has been identified as the key mediator of tumor-associated angiogenesis; thus, it is the most well-characterized and is the key target in antiangiogenic therapy.[34,35] Agents such as antibodies and soluble receptor constructs have been developed to target the VEGF system and Avastin (bevacizumab) has emerged as the leading antiangiogenic agent. Avastin is a recombinant humanized monoclonal antibody to VEGF-A, and is used in conjunction with chemotherapy for the treatment of metastatic cancer.[34,36,37] Interleukin-8 (*IL-8*) is expressed in many cancerous cell types, affecting proliferation and migration of cancer cells and tumor angiogenesis and metastasis, and studies have shown that highly metastatic solid tumors constitutively express *IL-8*.[38–41] Overexpression of *IL-8* has been found to be associated with VEGF-independent, tumor-associated angiogenesis; thus, *IL-8* may be the key to elucidating cancer resistance against anti-VEGF therapy.[38,42–44]

In this study, we aimed to investigate the effect of 3D architecture and tumor–stroma interaction on the angiogenic factor secretion profile of U2OS osteosarcoma cells by coculturing the tumor cells with immortalized fibroblasts or human umbilical vein endothelial cells (HUVECs). The effects ascribed by either stromal cell types in the coculture model were teased by labeling the osteosarcoma cells in a subset analysis. Transwell® migration assays were also conducted for U2OS cells grown in 2D and 3D monocultures or fibroblast coculture systems to investigate the physiological effect of upregulated angiogenic factors on endothelial cell migration. We also tested out anti-IL-8 and anti-VEGF-A therapies on these models to investigate the role of 3D culture and the coculture of tumor cells with fibroblasts on the efficacy of antiangiogenic treatments. Our findings reveal that the coculture of U2OS cells with immortalized fibroblasts resulted in a more profound effect ascribable to *IL-8* as opposed to VEGF-A in 3D culture, leading to an increase in the migration of HUVECs toward the 3D tumor constructs and sensitivity to anti-IL-8 therapy.

Materials and Methods

Fabrication of 3D silk scaffolds

Porous silk sponges were fabricated by freeze drying according to a previously published protocol.[14] Silk fibroin from *Bombyx mori* silkworms was degummed using a solution consisting of 0.25% (w/v) sodium carbonate and 0.25% (w/v) sodium dodecyl sulfate at 98°C for an hour while stirring (PC-420D; Corning). This process was repeated once. The silk fibroin was dissolved in a ternary solvent consisting of calcium chloride, ethanol, and distilled water in a molar ratio of 1:2:8 at 10% (w/v) concentration in a water bath maintained at 60–65°C. The solution was dialyzed overnight in distilled water and the concentration was calculated from its dry weight. The silk solution was diluted to 3% (w/v), placed in petri dishes, and freeze-dried (Epsilon 1–4 LSC; Christ) overnight to form porous silk sponges. The sponges were then soaked in 90% methanol to convert the silk to the β-sheet structure and washed with distilled water. The sponges were cut into 5-mm discs with a height of 5 mm.

Cell culture

We cultured human female U2OS osteosarcoma cells (ATCC) in McCoy's 5A modified medium (Sigma-Aldrich) containing 15% fetal bovine serum and 1% penicillin/streptomycin. Human male bone marrow fibroblasts transformed with HPV-16 E6/E7 (CRL-11882; ATCC) were cultured in DMEM (ATCC) containing 10% fetal bovine serum and 1% penicillin/streptomycin. The cells were trypsinized and cocultured with U2OS osteosarcoma cells (ATCC) when confluent. Single-donor HUVECs (C2517A; Lonza) were cultured in supplemented EGM-2 (Lonza) and used in migration assays or cocultured with U2OS cells when confluent.

Transfection of U2OS cells with green fluorescent protein

We tagged U2OS cells with green fluorescent protein (GFP) for cell sorting. U2OS cells were plated at a density

of 2×10^4 U2OS cells per well in a 6-well culture plate and cultured for 18 h in complete McCoy's 5A modified medium (Sigma-Aldrich). About 2 mL of Moloney murine leukemia viral supernatant with the Retro-GFP vector (Retro-Easy Gene Expression System; Applied Biological Materials) and 20 μL of 0.8 mg/mL polybrene (Sigma-Aldrich) were added to each well for 9 h. The wells were washed with phosphate-buffered saline before a second hit was applied and left in the incubator overnight. The medium was replaced with fresh complete McCoy's 5A modified medium (Sigma-Aldrich) and the cells were allowed to culture for 2 days before being replaced with culture medium containing 0.5 μg/mL puromycin (Applied Biological Materials) selection marker. We sorted the cells using an FACSVantage SE flow cytometer (Becton Dickinson), and those found positive for GFP were collected and expanded in culture.

Coculture experiments

Our discovery that *IL-8* and VEGF-A are upregulated by 143.98.2 cells under 3D culture[14] prompted us to repeat the experiment using the U2OS cell line to ensure that the increase in angiogenic potential of osteosarcoma cells in 3D culture was not specific to the 143.98.2 cell line. We transfected U2OS cells with a GFP vector to allow for identification and sorting of the GFP^+ U2OS tumor cells from the surrounding stromal cells. To study the effect of coculture on the expression of angiogenic growth factors, we cocultured GFP^+ U2OS cells with immortalized human bone marrow fibroblasts transformed with HPV-16 E6/E7 of HUVECs. We cocultured U2OS cells with immortalized fibroblasts or HUVECs under either 2D or 3D culture conditions. In the standardized 2D baseline, 2×10^4 U2OS cells were seeded on a T-75 polystyrene flask and left to grow for 2 days to form cell clusters. About 2×10^5 stromal cells (immortalized fibroblasts or HUVECs) were then added to the T-75 flask containing the U2OS cell clusters and cultured in McCoy's 5A modified medium (Sigma-Aldrich) until they reached confluence. These unsorted cocultured cells were either treated with TRIzol reagent (Invitrogen) for RNA extraction or trypsinized and injected in the 3D silk scaffolds at a cell density of 0.5×10^6 cells per scaffold, and cultured for 7 days. U2OS-GFP cells were used for real-time polymerase chain reaction (RT-PCR) involving sorted U2OS cells cultured in 2D monolayers with the respective stromal cells.

Fluorescence-activated cell sorting of cocultured U2OS-GFP cells

For the experiments involving transfected U2OS cells cocultured with fibroblasts or HUVECs in 2D monolayers, the cells first underwent fluorescence-activated cell sorting (FACS) using an FACSVantage SE flow cytometer (Becton Dickinson), and those found positive for GFP were collected for RNA extraction.

Analysis of expression of angiogenic markers

The 3D seeded scaffolds were minced and 1 mL of TRIzol reagent (Invitrogen) was added for cell lysis. The treated scaffolds were then vortexed and left to stand at room temperature for 5 min before being centrifuged at 13,000 rpm for 15 min (Centrifuge 5810R; Eppendorf). The supernatant was transferred to a new tube and 200 μL of chloroform was added and left to stand for 5 min. The tubes were centrifuged at 13,000 rpm for 15 min and the upper aqueous phase was transferred to a new tube. One volume of 70% (v/v) ethanol was added and the mixture was applied to an RNeasy mini spin column (Qiagen). RNA extraction was done according to the manufacturer's instructions. cDNA was synthesized from using the iScript cDNA synthesis kit according to the manufacturer's instructions (Bio-Rad Laboratories). RT-PCR was conducted using the iQ SYBR Green Supermix (Bio-Rad Laboratories). The primers used are summarized in Table 1. Standard descriptive statistics were used; mean and standard deviation were determined with respect to *GAPDH*. Student's *t*-test was used to compare paired data sets. Statistical significance was accepted at $p < 0.05$.

Transwell migration assays

For the 2D monolayers, 0.5×10^6 U2OS cells or U2OS cocultured with immortalized fibroblasts were plated directly on the bottom chamber of a six-well Transwell plate with pore size of 8 μm (Corning). For the 3D tumor constructs, 0.5×10^6 U2OS cells or U2OS cocultured with immortalized fibroblasts were seeded in the silk scaffold, cultured for 7 days, and transferred to the lower chamber. For the control, 5.5 mL of complete McCoy's 5A modified medium (Sigma-Aldrich) was added to each well of the lower chamber, such that the medium was just able to touch the upper chamber. For the treated conditions, 1 μg/mL of anti-IL-8 monoclonal antibody (MAB208; R&D Systems)[45] or anti-VEGF-A monoclonal antibody (Avastin, Genentech) was added to the culture medium in the lower chamber. The cells were placed in the lower chamber for 24 h. One-third of a T-75 flask of HUVECs prestarved for 3 h in serum-free DMEM (Invitrogen) was plated onto each insert of the upper chamber and incubated for 6 h. The inserts were then removed and the unmigrated HUVECs on the top surface of the inserts were wiped off using sterile cotton buds soaked

Table 1. Table of Primers

Gene name	*Forward primer*	*Backward primer*
bFGF	5′-GGA GAA GAG CGA CCC TCA CAT CAA G-3′	5′-CCA GTT CGT TTC AGT GCC ACA TAC CAA-3′
GAPDH	5′-GAG TCA ACG GAT TTG GTC GT-3′	5′-CAT GGG TGG AAT CAT ATT GGA-3′
HIF-1α	5′-TCA CCA CAG GAC AGT ACA GGA TGC-3′	5′-CCA GCA AAG TTA AAG CAT CAG GTT CC-3′
IL-8	5′-CAC CGG AAG GAA CCA TCT CAC T-3′	5′-TCA GCC CTC TTC AAA AAC TTC TCC-3′
VEGF-A	5′-CTG CTG TCT TGG GTG CAT TGG-3′	5′-TCA CCG CCT CGG CTT GTC-3′

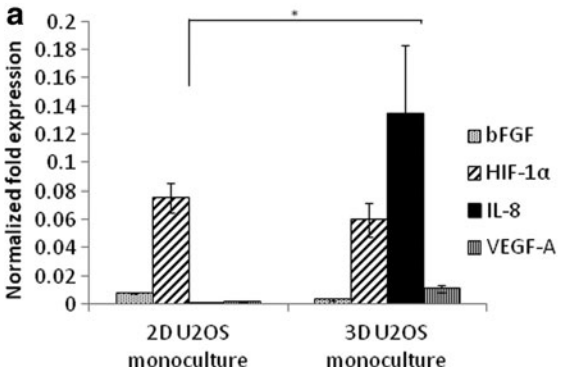

b

	Change in expression under 3D culture (%)
bFGF	-60.4
HIF-1α	-20.1
IL-8	20968.6
VEGF-A	500.1

FIG. 1. **(a)** Effect of substrate architecture on angiogenic factor expression by U2OS cells grown in two-dimensional (2D) T-75 flasks and three-dimensional (3D) silk scaffolds. **(b)** Percentage change in gene expression under 3D culture. *Statistically different at $p < 0.05$.

in PBS. The membranes were cut out and fixed in formalin overnight. For imaging, the membranes were soaked in 2 μg/mL DAPI stain for 10 min and viewed under a fluorescence microscope (Olympus IX71 microscope; WU filter).

Results

Upregulation of angiogenic factor expression by U2OS cells in 3D culture

The expression levels of angiogenic factors *bFGF*, *HIF-1α*, *IL-8*, and VEGF-A were investigated by conducting real-time quantitative PCR on day 7. U2OS cells under 3D culture were found to have a significant increase in the expression levels of *IL-8* and VEGF-A ($p = 0.049$ and 0.017, respectively) (Fig. 1a), with the upregulation of *IL-8* being tremendously higher than that of VEGF-A. *bFGF* was mildly downregulated for U2OS cells in 3D conditions ($p = 0.013$), while *HIF-1α* showed no significant difference compared with the 2D controls ($p = 0.17$). The percentage change in expression levels was tabulated in Figure 1b and there was only a 20.1% change in the expression of *HIF-1α*, indicating no biological significance. These results reflect those observed in our previous study using the 143.98.2 osteosarcoma cell line.[14]

Coculture of U2OS cells with immortalized fibroblasts increases angiogenic factor expression

We cocultured GFP$^+$ U2OS cells with immortalized human bone marrow fibroblasts to study the effect of fibroblast coculture on the expression of angiogenic growth factors (Fig. 2a). We isolated the GFP$^+$ U2OS cells using FACS and performed RT-PCR on the GFP$^+$ U2OS cells to

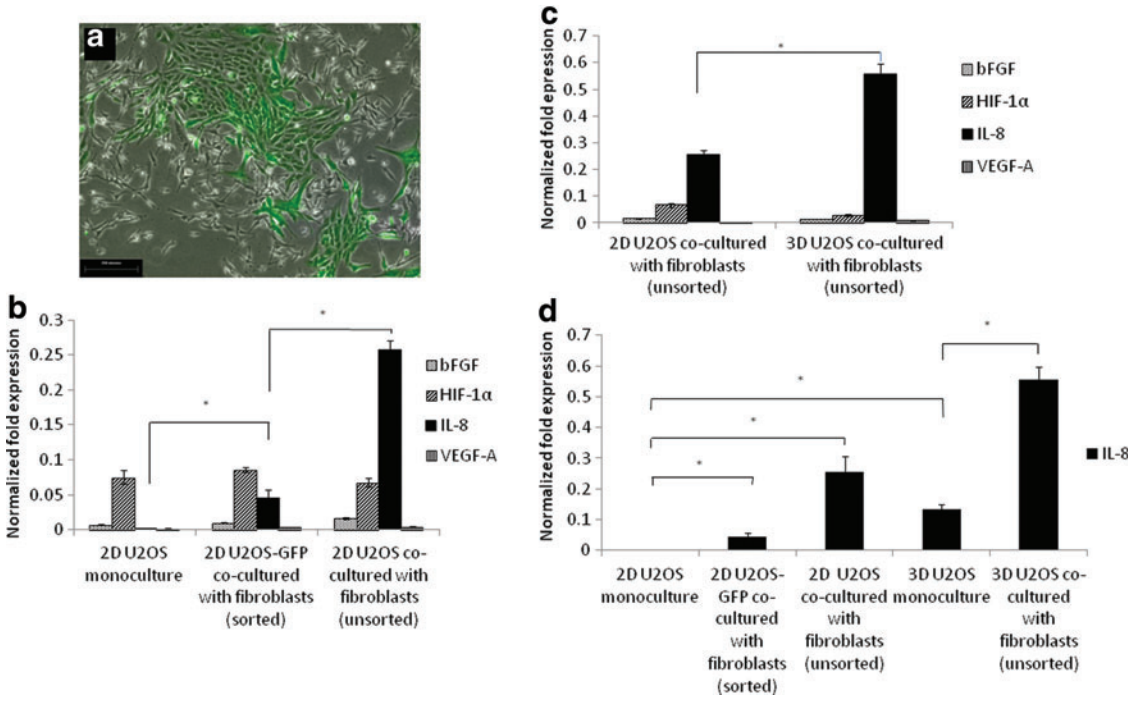

FIG. 2. **(a)** Microscopy images of U2OS cells transfected with green fluorescent protein (GFP) and cocultured with immortalized fibroblasts (100×, scale bar = 250 μm). **(b)** Effect of coculture with stromal fibroblasts on angiogenic factor secretion by 2D sorted U2OS cocultured with fibroblasts and 2D unsorted U2OS cocultured with fibroblasts. *Statistically different at $p < 0.05$. **(c)** Effect of coculture with stromal fibroblasts on angiogenic factor secretion by 2D unsorted U2OS cocultured with fibroblasts and 3D unsorted U2OS cocultured with fibroblasts. *Statistically different at $p < 0.05$. **(d)** Effect of 3D architecture and coculture on *IL-8* expression. Color images available online at www.liebertpub.com/tea

determine the cell-specific perturbations that occurred due to coculture exposure. These GFP-labeled isolates were designated as *sorted* moieties. When the sorted 2D coculture condition was compared with the U2OS cells in monoculture, there was a mild upregulation of both *bFGF* and VEGF-A, with $p = 0.032$ and 0.024, respectively (Fig. 2b). The expression level of *HIF-1α* was similar in both cases. U2OS cocultured with fibroblasts showed a marked upregulation of *IL-8* as compared with 2D monoculture ($p = 0.026$). RT-PCR on the unsorted coculture of U2OS cells with fibroblasts showed a further upregulation of all angiogenic factors, particularly *IL-8* ($p = 0.0059$, $0.024, < 0.001$, and 0.032 for *bFGF*, *HIF-1α*, *IL-8*, and VEGF-A, respectively), suggesting that the stromal fibroblasts produced additional angiogenic signals as well.

We investigated the combined effects of fibroblast coculture and 3D architecture on angiogenic factor expression. When U2OS and fibroblast cells were cocultured in the 3D scaffolds, VEGF-A was found to be only slightly upregulated while there was a striking upregulation of *IL-8*, indicating that the 3D architecture further induced the secretion of *IL-8* (Fig. 2c). We repeated the quantitative real-time PCR analysis for *IL-8* expression under the various culture conditions and found that the upregulation of *IL-8* under the 3D coculture model was higher than that of the unsorted 2D coculture and 3D monoculture models combined (Fig. 2d). Thus, the large upregulation of *IL-8* under the 3D coculture model was likely a synergistic outcome of 3D culture and 2D coculture, thereby highlighting the importance of the 3D architecture in the interaction between different cell types and populations.

Coculture of U2OS cells with HUVECs suppressed angiogenic factor expression in 3D models

We cocultured U2OS cells with HUVECs to study the effect of direct interaction with endothelial cells on the angiogenic potential of tumor cells. There was no significant upregulation of VEGF-A following 2D coculture for both the sorted and unsorted conditions ($p = 0.16$ and 0.32, respectively). HUVEC coculture also did not seem to play a major role in *IL-8* expression in 2D culture, with $p = 0.076$ for the sorted condition and $p = 0.014$ for the unsorted condition (Fig. 3a). There was a significant upregulation of both *IL-8* and VEGF-A in the 3D HUVEC coculture condition as compared with the 2D coculture study ($p = 0.024$ and 0.0027, respectively), highlighting the role of 3D culture on angiogenic factor expression (Fig. 3b). However, this was less than the levels of *IL-8* and VEGF-A expression under the 3D monoculture condition. HUVEC coculture acts

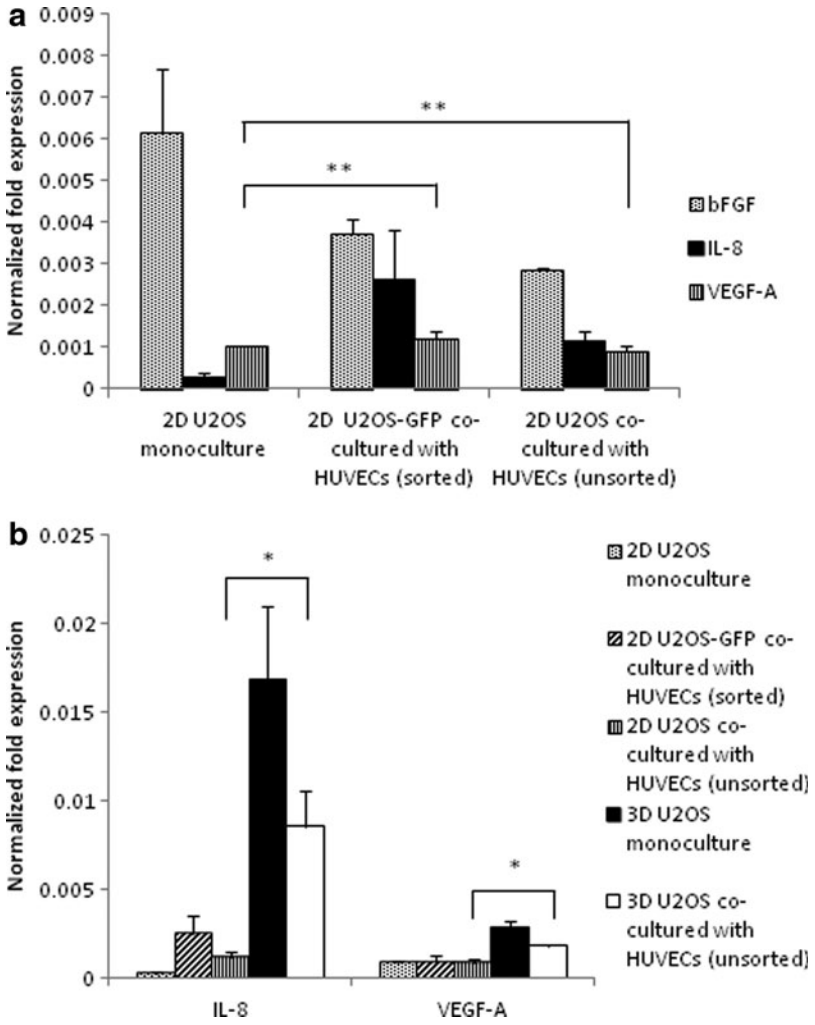

FIG. 3. **(a)** Effect of coculture with human umbilical vein endothelial cells (HUVECs) on angiogenic factor secretion by 2D U2OS monoculture, 2D GFP-sorted U2OS cocultured with HUVECs, and 2D unsorted U2OS cocultured with HUVECs. **Statistically similar at $p > 0.05$. **(b)** Upregulation of *IL-8* and VEGF-A in 3D coculture with HUVECs. *Statistically different at $p < 0.05$.

as a control in these experiments, showing that coculture in itself does not dictate an increase in angiogenic potential. Instead, the changes in the levels of angiogenic factor expression that result from coculture depend on the type of stromal cells that the tumor cells are cultured with, as evidenced from the modulation of angiogenic factor expression with fibroblast and HUVEC coculture.

Migration of HUVECs through Transwell inserts under the influence of angiogenic factors secreted by tumor constructs

Avastin is a recombinant humanized monoclonal antibody to VEGF-A (anti-VEGF-A). However, therapies involving Avastin have only shown modest clinical success. Likewise, treatment of the 3D tumor constructs with Avastin only resulted in a slight decrease in HUVEC migration (Fig. 4a). In contrast, a significant drop in HUVEC migration across the Transwell insert was observed when the 3D monoculture model was treated with anti-IL-8 monoclonal antibody. This implies that *IL-8* may play a larger role in endothelial cell migration, as compared to VEGF-A. The results obtained using the Transwell migration assays also demonstrate the physiological effect of *IL-8* on tumor-associated angiogenesis and suggest that the emphasis on anti-VEGF-A therapy should be shifted to an emphasis on anti-IL-8 therapy in clinical application.

Anti-IL-8 monoclonal antibody was tested on the coculture models. For the control conditions, there was a statistically significant increase in HUVEC migration under the influence of the 3D monoculture tumor construct as compared with the 2D model, possibly as a result of the

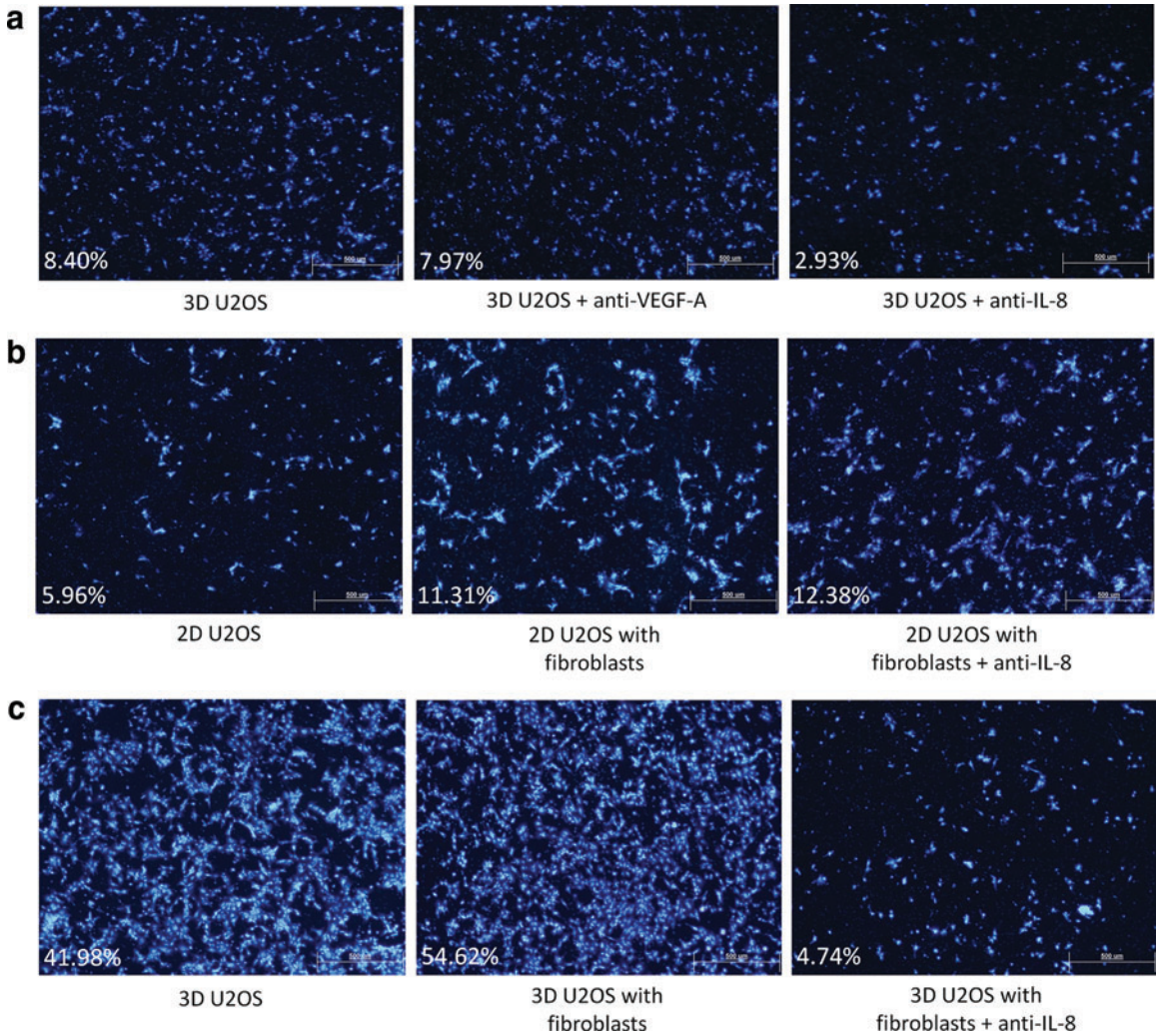

FIG. 4. HUVEC migration through Transwell® inserts. **(a)** HUVEC migration through the Transwell inserts for untreated 3D monoculture (left), 3D monoculture treated with 1 μg/mL anti-VEGF-A monoclonal antibody (center), and 3D monoculture treated with 1 μg/mL anti-IL-8 monoclonal antibody (right); **(b)** 2D monoculture (left), 2D cocultured with fibroblasts (center), and 2D cocultured with fibroblasts treated with 1 μg/mL anti-IL-8 monoclonal antibody (right); and **(c)** 3D monoculture (left), 3D cocultured with fibroblasts (center), and 3D cocultured with fibroblasts treated with 1 μg/mL anti-IL-8 monoclonal antibody (right) (DAPI, 40×, scale bar = 500 μm). The percentage of the total membrane area covered by the migrated HUVECs is given for each condition. Comparisons should only be made horizontally, as different batches of HUVECs were used for each set of experiments. Color images available online at www.liebertpub.com/tea

upregulation of *IL-8* expression under the 3D culture condition (Fig. 4b, c). Coculture with fibroblasts led to a slight increase in HUVEC migration for both the 2D and 3D models, which follows the trends in the *IL-8* expression profiles seen in Figure 2d, and treatment of these coculture models with anti-IL-8 monoclonal antibody had no effect on the 2D coculture model, while the migration of HUVECs toward the 3D coculture model was dramatically reduced. This highlights the importance of the architecture in which the tumor cells are cultured in on the efficacy of anti-angiogenic therapy, and makes a strong case for the use of anti-IL-8 therapy in the prevention of tumor-associated angiogenesis.

Discussion

The angiogenic factors *bFGF*, *IL-8*, and VEGF-A play key roles in the modulation of angiogenesis, while *HIF-1α* induces an angiogenic response through VEGF-A during hypoxia. The importance of these factors has been established in our previous study and also by other groups.[14,41,46,47] The upregulation of *IL-8* and VEGF-A by U2OS cells grown in the 3D silk scaffolds is similar to that obtained using 143.98.2 osteosarcoma cells, the results of which have been published previously.[14] This earlier study also showed that the *Bombyx mori* silk substrate does not influence the expression of angiogenic factors and appears to be as inert as conventional culture substrates. This highlights the validity of the 3D tumor model proposed as opposed to the material it is made from, and it is highly likely that these silk scaffolds will find application in epithelial cancers, such as breast and prostate. The upregulation of *IL-8* in 2D coculture systems is also in line with a previously published study that demonstrated a twofold increase in *IL-8* expression levels in LS174T colon cancer cell lines cocultured with colon-derived fibroblasts.[48] *IL-8* has been reported to act on VEGFR-2, resulting in the upregulation of mRNA and protein expression of VEGF-A in a process independent of *HIF-1α*.[49,50] *IL-8* has also been established to have the ability to promote tumor-associated angiogenesis through a pathway independent of VEGF-A, suggesting that upregulation of *IL-8* might result in more aggressive angiogenesis.[38,44]

Recent studies have suggested that enhanced *IL-8* expression may be related to changes in cell morphology. The mechanical architecture of the ECM influences cell–matrix interaction and focal adhesions, and a change from 2D to 3D culture would lead to alterations in Rho GTPase signaling involved in the transmission of mechanical forces through the cytoskeleton.[51] Alteration of the actin cytoskeleton has been found to lead to the differential activation of NFκB, a transcription factor that induces *IL-8* expression.[52] It has been postulated that *IL-8* expression, integrin engagement, and cell morphology are interrelated, thereby resulting in the upregulation of *IL-8* under 3D culture seen in this study.[47] There has been increasing evidence that *IL-8* has a much more crucial role in tumor-associated angiogenesis than previously assumed; thus, the resulting upregulation of *IL-8* in these 3D monoculture and fibroblast coculture tumor models may offer a more physiologically relevant model for drug testing.

The results obtained using the Transwell migration assays for the comparison study between anti-VEGF-A and anti-IL-8 treatments on HUVEC migration suggest that *IL-8* plays a more crucial role in endothelial cell migration than VEGF-A and highlights the importance of the 3D architecture on the predictive accuracy of *in vitro* studies. The data help to model the physiological effect of *IL-8* on tumor-associated angiogenesis and make a good case for the use of anti-IL-8 therapy in the prevention of neovascularization. VEGF-A and anti-VEGF therapies have been widely established and traditionally targeted in cancer research; however, these results suggest that anti-IL-8 treatment modalities should be approached and studied further. While the gains from anti-VEGF-A therapy have been modest, an alternative antiangiogenic initiative in solid cancer control should be pursued. Anti-VEGF and anti-IL-8 combination therapy also has great potential in future antiangiogenic studies. Multiple small-molecule inhibitors and humanized monoclonal antibodies are now emerging as possible therapeutic approaches to attenuate *IL-8* and its receptors, so as to curb disease progression and modulate the response to combination chemotherapy in preclinical models.[42] However, targeting *IL-8* expression through either humanized monoclonal antibodies against *IL-8* or small-interfering RNA strategies may not necessarily attenuate the effects of other CXC chemokines in the tumor microenvironment. Thus, it has been postulated that receptor-targeted strategies that eliminate the entire cascade of chemokine signaling may prove to be more efficacious than agents that solely dampen the effects of *IL-8*.[53] CXCR1 and CXCR2 have also been suggested as prime targets for small-molecule inhibitors, and the inhibition of CXCR2 in the tumor microenvironment has been shown to profoundly affect colon cancer growth and angiogenesis, and even increasing intratumoral necrosis.[42,54–58]

In conclusion, the coculture of U2OS cells with immortalized fibroblasts led to the upregulation of angiogenic factors, particularly *IL-8*. This was especially pronounced when combined with the effects of the architecture of the 3D silk scaffold. On the other hand, coculture with endothelial cells did not lead to increased angiogenic factor production, and instead led to a downregulation of *IL-8* and VEGF-A under 3D culture conditions. The importance of fibroblast coculture and *IL-8* production was highlighted when the migration of HUVECs through the Transwell polycarbonate inserts increased for the 3D and coculture models, and the targeted inhibition of *IL-8* greatly reduced HUVEC migration despite the presence of VEGF-A. Thus, this 3D tumor coculture model is likely a better preclinical model for drug testing, and stands to help bridge the gap between conventional 2D models and animal xenograft models. This research also has significant implications on the use of antiangiogenic therapy targeting VEGF-A in combination with chemotherapy in the clinical setting.

Acknowledgments

The authors thank A/Prof. Michael Raghunath from the NUSTEP Tissue Modulation Laboratory for providing the HUVECs used in this study. This study was supported by the MOE Academic Research Fund (Grant T13-1001-P04).

Disclosure Statement

No competing financial interests exist.

References

1. Lorusso, G., and Rüegg, C. The tumor microenvironment and its contribution to tumor evolution toward metastasis. Histochem Cell Biol **130,** 1091, 2008.
2. Verbridge, S.S., Chandler, E.M., and Fischbach, C. Tissue-engineered three-dimensional tumor models to study tumor angiogenesis. Tissue Eng Part A **16,** 2147, 2010.
3. Hutmacher, D.W., *et al.* Can tissue engineering concepts advance tumor biology research? Trends Biotechnol **28,** 125, 2010.
4. Hutmacher, D.W., *et al.* Translating tissue engineering technology platforms into cancer research. J Cell Mol Med **13,** 1417, 2009.
5. Verbridge, S.S., *et al.* Oxygen-controlled three-dimensional cultures to analyze tumor angiogenesis. Tissue Eng Part A **16,** 2133, 2010.
6. Kim, J.B., Stein, R., and O'Hare, M.J. Three-dimensional in vitro tissue culture models of breast cancer—a review. Breast Cancer Res Treat **85,** 281, 2004.
7. Liu, X., Holzwarth, J.M., and Ma, P.X. Functionalized synthetic biodegradable polymer scaffolds for tissue engineering. Macromol Biosci **12,** 911, 2012.
8. Middleton, J.C., and Tipton, A.J. Synthetic biodegradable polymers as orthopedic devices. Biomaterials **21,** 2335, 2000.
9. Meyer, F., *et al.* Effects of lactic acid and glycolic acid on human osteoblasts: a way to understand PLGA involvement in PLGA/calcium phosphate composite failure. J Orthop Res **30,** 864, 2012.
10. Zhou, C.Z., *et al.* Silk fibroin: structural implications of a remarkable amino acid sequence. Proteins **44,** 119, 2001.
11. Ki, C.S., *et al.* Development of 3-D nanofibrous fibroin scaffold with high porosity by electrospinning: implications for bone regeneration. Biotechnol Lett **30,** 405, 2008.
12. Altman, G.H., *et al.* Silk-based biomaterials. Biomaterials **24,** 401, 2003.
13. Wang, Y., *et al.* Stem cell-based tissue engineering with silk biomaterials. Biomaterials **27,** 6064, 2006.
14. Tan, P.H., *et al.* Three-dimensional porous silk tumor constructs in the approximation of in vivo osteosarcoma physiology. Biomaterials **32,** 6131, 2011.
15. Talukdar, S., *et al.* Engineered silk fibroin protein 3D matrices for in vitro tumor model. Biomaterials **32,** 2149, 2011.
16. Goldstein, R.H., *et al.* Human bone marrow-derived MSCs can home to orthotopic breast cancer tumors and promote bone metastasis. Cancer Res **70,** 10044, 2010.
17. Moreau, J.E., *et al.* Tissue-engineered bone serves as a target for metastasis of human breast cancer in a mouse model. Cancer Res **67,** 10304, 2007.
18. Kwon, H., *et al.* Development of an in vitro model to study the impact of BMP-2 on metastasis to bone. J Tissue Eng Regen Med **4,** 590, 2010.
19. Kundu, S.C., *et al.* Invited review nonmulberry silk biopolymers. Biopolymers **97,** 455, 2012.
20. Huang, C.P., *et al.* Engineering microscale cellular niches for three-dimensional multicellular co-cultures. Lab Chip **9,** 1740, 2009.
21. Castelló-Cros, R., *et al.* Staged stromal extracellular 3D matrices differentially regulate breast cancer cell responses through PI3K and beta1-integrins. BMC Cancer **9,** 94, 2009.
22. Hartman, O., *et al.* Microfabricated electrospun collagen membranes for 3-D cancer models and drug screening applications. Biomacromolecules **10,** 2019, 2009.
23. Li, H., Fan, X., and Houghton, J. Tumor microenvironment: the role of the tumor stroma in cancer. J Cell Biochem **101,** 805, 2007.
24. Kalluri, R., and Zeisberg, M. Fibroblasts in cancer. Nat Rev Cancer **6,** 392, 2006.
25. Bhowmick, N.A., Neilson, E.G., and Moses, H.L. Stromal fibroblasts in cancer initiation and progression. Nature **432,** 332, 2004.
26. Mbeunkui, F., and Johann, D.J. Cancer and the tumor microenvironment: a review of an essential relationship. Cancer Chemoth Pharm **63,** 571, 2009.
27. Tlsty, T.D., and Coussens, L.M. Tumor stroma and regulation of cancer development. Annu Rev Pathol **1,** 119, 2006.
28. Yang, X., Takano, Y., and Zheng, H.C. The pathobiological features of gastrointestinal cancers (Review). Oncol Lett **3,** 961, 2012.
29. Kirsch, M., Schackert, G., and Black, P.M. Angiogenesis, metastasis, and endogenous inhibition. J Neurooncol **50,** 173, 2000.
30. Konno, H., Yamamoto, M., and Ohta, M. Recent concepts of antiangiogenic therapy. Surg Today **40,** 494, 2010.
31. Park, S.Y., *et al.* Norepinephrine induces VEGF expression and angiogenesis by a hypoxia-inducible factor-1alpha protein-dependent mechanism. Int J Cancer **128,** 2306, 2011.
32. Mashiko, R., *et al.* Hypoxia-inducible factor 1alpha expression is a prognostic biomarker in patients with astrocytic tumors associated with necrosis on MR image. J Neurooncol **102,** 43, 2011.
33. Eggert, A., *et al.* High-level expression of angiogenic factors is associated with advanced tumor stage in human neuroblastomas. Clin Cancer Res **6,** 1900, 2000.
34. Grothey, A., and Galanis, E. Targeting angiogenesis: progress with anti-VEGF treatment with large molecules. Nat Rev Clin Oncol **6,** 507, 2009.
35. Zhao, M., *et al.* JAK2/STAT3 signaling pathway activation mediates tumor angiogenesis by upregulation of VEGF and bFGF in non-small-cell lung cancer. Lung Cancer **73,** 366, 2011.
36. Small, A.C., and Oh, W.K. Bevacizumab treatment of prostate cancer. Expert Opin Biol Ther **12,** 1241, 2012.
37. Ferrarotto, R., and Hoff, P.M. Antiangiogenic drugs for colorectal cancer: exploring new possibilities. Clin Colorectal Cancer **12,** 1, 2013.
38. Ning, Y., *et al.* Interleukin-8 is associated with proliferation, migration, angiogenesis and chemosensitivity in vitro and in vivo in colon cancer cell line models. Int J Cancer **128,** 2038, 2011.
39. Xie, K. Interleukin-8 and human cancer biology. Cytokine Growth Factor Rev **12,** 375, 2001.
40. Xu, L., and Fidler, I.J. Interleukin 8: an autocrine growth factor for human ovarian cancer. Oncol Res **12,** 97, 2000.
41. Huang, S., *et al.* Fully humanized neutralizing antibodies to interleukin-8 (ABX-IL8) inhibit angiogenesis, tumor growth, and metastasis of human melanoma. Am J Pathol **161,** 125, 2002.
42. Ning, Y., and Lenz, H.J. Targeting IL-8 in colorectal cancer. Expert Opin Ther Targets **16,** 491, 2012.
43. Li, A., *et al.* IL-8 directly enhanced endothelial cell survival, proliferation, and matrix metalloproteinases production and regulated angiogenesis. J Immunol **170,** 3369, 2003.

44. Matsuo, Y., *et al.* CXCL8/IL-8 and CXCL12/SDF-1alpha co-operatively promote invasiveness and angiogenesis in pancreatic cancer. Int J Cancer **124,** 853, 2009.
45. Li, K.C., *et al.* The role of IL-8 in the SDF-1alpha/CXCR4-induced angiogenesis of laryngeal and hypopharyngeal squamous cell carcinoma. Oral Oncol **48,** 507, 2012.
46. Fischbach, C., *et al.* Engineering tumors with 3D scaffolds. Nature methods **4,** 855, 2007.
47. Fischbach, C., *et al.* Cancer cell angiogenic capability is regulated by 3D culture and integrin engagement. Proc Natl Acad Sci U S A **106,** 399, 2009.
48. Dolznig, H., *et al.* Modeling colon adenocarcinomas in vitro a 3D co-culture system induces cancer-relevant pathways upon tumor cell and stromal fibroblast interaction. Am J Pathol **179,** 487, 2011.
49. Martin, D., Galisteo, R., and Gutkind, J.S. CXCL8/IL8 stimulates vascular endothelial growth factor (VEGF) expression and the autocrine activation of VEGFR2 in endothelial cells by activating NFkappaB through the CBM (Carma3/Bcl10/Malt1) complex. J Biol Chem **284,** 6038, 2009.
50. He, W., *et al.* High tumor levels of IL6 and IL8 abrogate preclinical efficacy of the gamma-secretase inhibitor, RO4929097. Mol Oncol **5,** 292, 2011.
51. Provenzano, P.P., and Keely, P.J. Mechanical signaling through the cytoskeleton regulates cell proliferation by coordinated focal adhesion and Rho GTPase signaling. J Cell Sci **124,** 1195, 2011.
52. Nemeth, Z.H., *et al.* Disruption of the actin cytoskeleton results in nuclear factor-kappaB activation and inflammatory mediator production in cultured human intestinal epithelial cells. J Cell Physiol **200,** 71, 2004.
53. Waugh, D.J., and Wilson, C. The interleukin-8 pathway in cancer. Clin Cancer Res **14,** 6735, 2008.
54. Singh, S., Sadanandam, A., and Singh, R.K. Chemokines in tumor angiogenesis and metastasis. Cancer Metastasis Rev **26,** 453, 2007.
55. Bertini, R., *et al.* Noncompetitive allosteric inhibitors of the inflammatory chemokine receptors CXCR1 and CXCR2: prevention of reperfusion injury. Proc Natl Acad Sci U S A **101,** 11791, 2004.
56. Dwyer, M.P., *et al.* Discovery of 2-hydroxy-N,N-dimethyl-3-{2-[[(R)-1-(5-methylfuran-2-yl)propyl]amino]-3,4-dioxocyclobut-1-enylamino}benzamide (SCH 527123): a potent, orally bioavailable CXCR2/CXCR1 receptor antagonist. J Med Chem **49,** 7603, 2006.
57. Varney, M.L., *et al.* Small molecule antagonists for CXCR2 and CXCR1 inhibit human colon cancer liver metastases. Cancer Lett **300,** 180, 2011.58. Lee, Y.S., *et al.* Interleukin-8 and its receptor CXCR2 in the tumour microenvironment promote colon cancer growth, progression and metastasis. Br J Cancer **106,** 1833, 2012.

Address correspondence to:
Saminathan Suresh Nathan, MD
Musculoskeletal Oncology Research Laboratories
Department of Orthopaedic Surgery
National University of Singapore
NUHS Tower Block, Level 11
1E Kent Ridge Road
Singapore 119228
Singapore

E-mail: dosssn@nus.edu.sg

Received: April 23, 2013
Accepted: December 23, 2013
Online Publication Date: April 29, 2014